



The urban heat island effect and city contiguity

Neil Debbage ^{*}, J. Marshall Shepherd

Department of Geography, University of Georgia, Athens, GA 30602, USA



ARTICLE INFO

Article history:

Received 4 January 2015

Received in revised form 3 August 2015

Accepted 9 August 2015

Available online xxxx

Keywords:

Urban heat island

Urban morphology

Spatial contiguity

Urban planning

PRISM

Spatial metrics

ABSTRACT

The spatial configuration of cities can affect how urban environments alter local energy balances. Previous studies have reached the paradoxical conclusions that both sprawling and high-density urban development can amplify urban heat island intensities, which has prevented consensus on how best to mitigate the urban heat island effect via urban planning. To investigate this apparent dichotomy, we estimated the urban heat island intensities of the 50 most populous cities in the United States using gridded minimum temperature datasets and quantified each city's urban morphology with spatial metrics. The results indicated that the spatial contiguity of urban development, regardless of its density or degree of sprawl, was a critical factor that influenced the magnitude of the urban heat island effect. A ten percentage point increase in urban spatial contiguity was predicted to enhance the minimum temperature annual average urban heat island intensity by between 0.3 and 0.4 °C. Therefore, city contiguity should be considered when devising strategies for urban heat island mitigation, with more discontiguous development likely to ameliorate the urban heat island effect. Unraveling how urban morphology influences urban heat island intensity is paramount given the human health consequences associated with the continued growth of urban populations in the future.

© 2015 Elsevier Ltd. All rights reserved.

1. Introduction

Urban areas are increasingly important, as 52% of the world population and 76% of individuals in developed countries resided in cities as of 2013 ([Population Reference Bureau, 2013](#)). Since urban population growth is projected to continue, with approximately 67% of the world population being urban dwellers by 2050 ([United Nations, 2012](#)), it is imperative to work towards a better understanding of the complex processes found at the intersection of urbanization, climate and human health.

The enhanced anthropogenic heat emissions, reduced evaporative cooling, increased surface roughness, lower surface albedos and narrow urban canyon geometry associated with cities often results in the formation of urban heat islands (UHIs), particularly at night, as urban air temperatures are higher relative to the natural surroundings ([Oke, 1982](#)). Increasingly warm urban environments pose serious threats to human health ([Patz, Campbell-Lendrum, Holloway, & Foley, 2005](#); [McMichael, Woodruff, & Hales, 2006](#)) because they amplify near-surface ozone concentrations ([Cardelino & Chameides, 1990](#)), reduce air quality ([Sarrat, Lemonsu, Masson, & Guedalia, 2006](#)), enhance anthropogenic energy consumption ([Rosenfeld, Akbari, Romm, & Pomerantz, 1998](#)) and increase heat related fatalities by magnifying the severity of heat waves ([Zhou & Shepherd, 2010](#); [Stone, 2012](#); [Li &](#)

[Bou-Zeid, 2013](#)). Partially due to the UHI effect, extreme heat events on average are responsible for more climate-related fatalities than any other form of severe weather ([Johnson & Wilson, 2009](#); [Stone, Hess, & Frumkin, 2010](#)).

While there is general agreement that cities fundamentally alter local energy balances ([Arnfield, 2003](#); [Souch & Grimmond, 2006](#)), how their spatial configurations influence the UHI effect is still debated. Traditionally, high-density urban development has been associated with greater UHI intensities since many of the mechanisms producing the UHI effect are often most pronounced within dense urban cores ([Oke, 1982, 1987](#)). [Oke and East \(1971\)](#) provided an early example of the linkages between city density and UHI intensity, as the UHI effect of Montreal was generally found to be most prominent in areas of particularly dense development.

However, more recent studies have concluded paradoxically that both more sprawling ([Stone & Rodgers, 2001](#); [Stone, 2012](#)) and denser ([Coutts, Beringer, & Tapper, 2007](#); [Martilli, 2014](#); [Schwarz & Manceur, 2014](#)) city configurations can result in more intense UHIs. Sprawl, typically defined as low-density, leapfrog urban expansion consisting of segregated land uses and widespread commercial strip development ([Burchell et al., 1998](#)), can exacerbate UHI intensities since it results in more land clearances, impervious surfaces and excess heat generated per capita when compared to higher density development ([Stone & Rodgers, 2001](#); [Stone, 2012](#)). Sprawling configurations also contribute to the UHI intensity observed within the city center since the cooling influence of the UHI circulation ([Haeger-Eugensson & Holmer, 1999](#)) is impaired by the warm suburban periphery ([Stone, 2012](#)). In contrast,

* Corresponding author.

E-mail address: debbage@uga.edu (N. Debbage).

other studies have continued to document the connections between higher densities and more intense UHIs, primarily due to the urban canyon geometry altering heat storage release, using in-situ observations (Coutts et al., 2007), modeling (Martilli, 2014) and remote sensing (Schwarz & Manceur, 2014).

Although some of these discrepancies are partially attributable to the particular cities analyzed in the various studies, the specific type of UHI evaluated and the diverse methodologies developed to quantify UHI intensity as well as urban form, the overall lack of consensus regarding the relationships between city configuration and the UHI effect has implications that extend beyond the realm of urban climatology. Specifically, the conflicting findings pose a serious urban planning dilemma: is high-density urban development a viable UHI mitigation strategy (Emmanuel & Fernando, 2007; Stone, 2012) or will densification actually make cities less livable due to an intensification of the UHI effect (Coutts et al., 2007; Martilli, 2014; Schwarz & Manceur, 2014)? The importance of resolving this question is highlighted by the recent calls for additional empirical research to help clarify the ambiguous influence of city configuration on the UHI effect (Ewing & Rong, 2008; Martilli, 2014).

By examining the UHI intensities of 50 cities with various urban morphologies, this study aims to evaluate the degree to which city configuration influences the UHI effect and attempts to resolve the apparent sprawl-density dichotomy concerning the most appropriate urban form for UHI mitigation. The following section outlines the data sources and methodologies used to investigate the relationships between urban morphology and the UHI effect. The results of the analysis and a discussion are presented in Section 3. Finally, the broader

urban planning implications and general conclusions of the research are summarized in Section 4.

2. Data and methods

2.1. Study area and methodology overview

The canopy UHI intensities and spatial configurations of the fifty most populous Metropolitan Statistical Areas (MSAs) in the contiguous United States, according to the 2010 US Census, were analyzed (Fig. 1). A MSA consists of at least one urban core with a population of 50,000 or greater and the adjacent counties that are socio-economically tied to that core, as determined by commuting data. In recognition of the methodological shortcomings associated with the urban–rural site comparison technique traditionally used to evaluate the UHI effect, most notably the subjective nature of selecting an urban and rural station as well as the inability to fully capture the heterogeneity of temperature within the urbanized area and the surrounding natural landscape (Peng et al., 2011; Jin, 2012), this study establishes a method for estimating UHI intensities that utilizes PRISM (Parameter-elevation Relationships on Independent Slopes Model) climate data (Daly et al., 2008). The spatial configurations of the cities were quantified using several spatial metrics that evaluated shape complexity, spatial contiguity, polycentrism and fragmentation. Bivariate and multivariate statistical techniques were then employed to analyze the relationships between urban morphology and UHI intensity. A more detailed explanation of these methodologies is provided in the following sections.

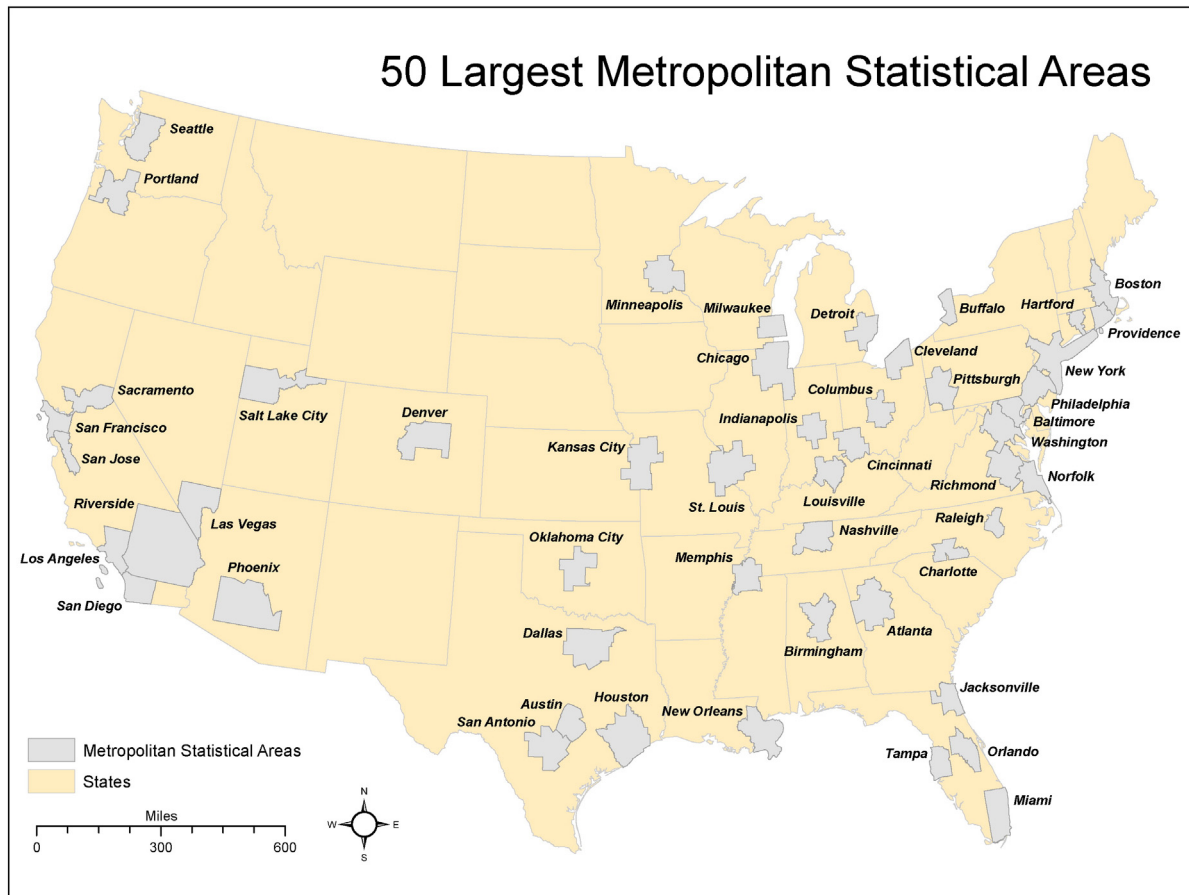


Fig. 1. Map of the MSAs included in the analysis. Approximately 54% of the United States population resided within the 50 most populous MSAs in 2010.

2.2. Datasets and derived variables

2.2.1. Urban heat island intensity estimation

A methodology that used PRISM climate data was developed to systematically estimate the canopy UHI intensities for each MSA (Daly et al., 2008). PRISM is an analytical model that creates gridded estimates by incorporating discrete measurements of climatic variables (e.g. temperature, precipitation, etc.), expert knowledge of complex climatic events (e.g. rain shadows, temperature inversions and coastal regimes) and a digital elevation model into a knowledge-based system. The gridded PRISM data has a resolution of approximately 4 km, which allows numerous grid points to exist within the urban areas of each MSA. Specifically, the PRISM products for annual and monthly average minimum temperature were used. The canopy UHI is most intense at night so minimum temperatures were analyzed rather than maximums or averages (Oke, 1982, 1987).

The PRISM minimum temperature datasets incorporate nearly 10,000 surface observations from over ten station networks across the United States to achieve the most comprehensive coverage possible. The primary limitation of using PRISM, or any similar gridded climate data product, is its dependency upon the density of the underlying station networks. This was less of an issue since the analysis focused on the urban environment, which is where station networks are typically denser. However, to ensure that station availability was not systematically biasing the UHI intensity estimates, the number of surface observations within each city that were potentially used during the PRISM interpolation process was determined. Additionally, the station availability within different land uses and land covers (LULCs) was analyzed to confirm that the urban areas of each city were being sampled representatively and that any minor over or under sampling differences between the cities were not biasing the UHI estimates. Sample representativeness was evaluated by calculating the ratio between the percentage of urban stations and the percentage of urban land cover for each city, where urban was defined by the four developed categories of the LULC dataset detailed in the following section.

The UHI intensities for each MSA were estimated by subtracting the average rural temperature from the average urban temperature (Eq. (1)). The average urban temperature was derived by averaging the temperatures of all the PRISM grid cells within the 2010 Census Urbanized Areas (UA) and Urban Clusters (UC) included in each MSA. UA, as defined by the US Census, contain at least 50,000 people and include one central urban core and the adjacent densely settled territory. UC are similar to UA except they must contain at least 2500 individuals. Since UA/UC are largely based on population density, some researchers (Sutton, Goetz, Fildes, Forster, & Ghosh, 2010; Bereitschaft & Debbage, 2013; Bereitschaft & Debbage, 2014) have used nighttime light intensity as an alternative method to delineate urbanized areas. However, the inclusion of non-residential urban land uses characterized by high levels of imperviousness within the 2010 US Census definition of UA/UC make them a more viable option since they are no longer determined solely by population data. A rural area outside the UA/UC included in each MSA was delineated using a buffer, and the average rural temperature was derived by averaging the temperatures of all the PRISM grid cells falling within this rural domain.

$$\text{UHI}^{\circ}\text{C} = \text{Tmin}_{\text{Urban Average}} - \text{Tmin}_{\text{Rural Average}} \quad (1)$$

Potential confounding factors (Stewart, 2011) were controlled for when defining the extent of the “rural” area for each MSA. For example, elevation changes and neighboring urban areas could distort the UHI estimates if the buffer used to define the rural domain included mountainous terrain or overlapped neighboring MSAs. A systematic rule-based system was developed to combat these potential biases. Firstly, a 50 km buffer around the UA/UC was created to define a preliminary rural area (Fig. 2A). A digital elevation model was incorporated to limit the defined rural domain to only those regions within ± 50 m

(Imhoff, Zhang, Wolfe, & Bounoua, 2010) of the average elevation of the UA/UC (Fig. 2B). Finally, any neighboring urban areas within the rural buffer were systematically excluded (Fig. 2C).

The urban domain and finalized rural domain (Fig. 2C), which controlled for elevation and neighboring urbanized areas, were used to estimate the UHI intensities for each month in 2010, the 2010 annual average UHI intensity and a longer-term annual average UHI intensity calculated from 2006 to 2010. The study focuses predominately on 2010 since the urban–rural boundaries used for the UHI intensity estimation were defined by 2010 US Census data. The longer-term average considered 2006 to 2010, as this five-year window enabled an appropriate comparison with the spatial metrics since they were derived from a 2006 LULC dataset. Finally, the usage of annual and monthly average UHI intensities, rather than daily or weekly estimates, helped capture the influence of city configuration on the UHI effect since urban morphologies are fairly persistent throughout a given year. Using a finer temporal resolution would be less suitable since daily variability in UHI intensity is more likely related to differing meteorological conditions than urban form itself.

2.2.2. Quantifying the spatial configurations of cities with spatial metrics

LULC data obtained from the US Geological Survey (USGS) Multi-Resolution Land Characteristics Consortium (MRLC) served as the foundation for calculating a set of spatial metrics. The MRLC maintains the National Land Cover Database (NLCD), which is a series of LULC datasets based primarily on the unsupervised classification of Landsat imagery. The NLCD 2006, which has a spatial resolution of 30 m and an overall accuracy of 78% (Wickham et al., 2013), was used in this study. It includes 20 LULC categories that are based on a classification scheme modified from the Anderson Land Cover Classification System. In order to investigate how different degrees of urbanization influence the UHI effect, the spatial metrics were calculated individually for each of the four urban categories included in the NLCD 2006.

Developed open space (Class 21) is the least urban of the NLCD 2006 developed land classes, as it includes pixels where impervious surfaces account for less than 20% of the total cover. This class typically consists of single-family homes on large parcels as well as vegetation planted within an urban context for erosion control, esthetic purposes or recreation. The low-intensity development (Class 22) and medium-intensity development (Class 23) categories incorporate pixels with higher levels of imperviousness, 20–49% and 50–79% of the total cover respectively, but both correspond predominately to single-family housing units on smaller lots. Finally, high-intensity development (Class 24) encompasses pixels with 80–100% impervious surface coverage and includes areas where people live or work in large quantities (Homer, Huang, Yang, Wylie, & Coan, 2004; Fry et al., 2011). In addition to calculating the spatial metrics for the four urban categories (Classes 21–24), the remaining 11 LULC classes included in NLCD 2006 were also analyzed. The LULC classes do not sum to 20 because four of the categories exist only in Alaska and one, perennial snow, did not occur within any of the MSAs.

Due to the focus on urban climatic processes, the LULC data were not analyzed for entire MSAs because in some cases the MSA boundary includes large amounts of rural land cover (Galster et al., 2001). Overbounded metropolitan counties, those whose administrative boundaries include not only an urban center but also contain large rural expanses not related to the urban core, are partially responsible for this incongruity between urban land use and MSA demarcation. In order to analyze only the urban environments, the LULC data within the UA/UC included in each MSA was extracted. These are the same UA/UC used to derive the average urban temperatures for the UHI intensity estimations. Overall, focusing on the LULC data within the UA/UC of each MSA established a much more appropriate landscape extent for the spatial metric calculations.

The public domain software FRAGSTATS (McGarigal, Cushman, & Ene, 2012) was used to compute the individual spatial metrics.

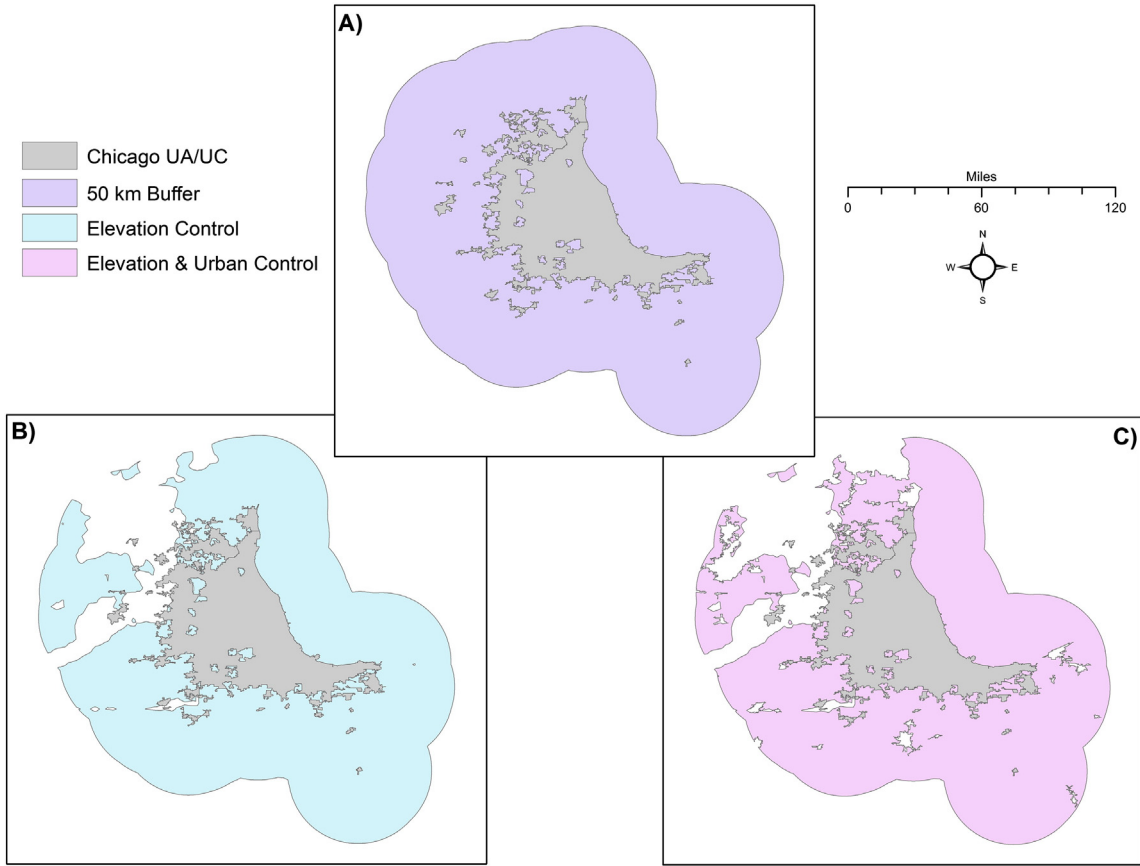


Fig. 2. An example from Chicago, Illinois of the urban and rural domains used to derive the average urban temperature and average rural temperature for the UHI intensity estimates. The 2010 US Census UA/UC defined the urban domain. The UA/UC are surrounded by the initial 50 km rural domain (A), the elevation control rural domain (B) and the finalized rural domain that controlled for elevation and did not contain any neighboring urban areas (C).

Although one specific suite of spatial metrics for analyzing urban environments has not been established (Herold, Couclelis, & Clarke, 2005), reviewing the relevant literature helped identify some of the most frequently utilized metrics to quantify urban form (Herold, Scepan, & Clarke, 2002; Herold, Goldstein, & Clarke, 2003; Ji, Ma, Twibell, & Underhill, 2006; Huang, Lu, & Sellers, 2007; Jat, Garg, & Khare, 2008; Bereitschaft & Debbage, 2014). Since spatial metrics have been less commonly used to analyze the specific relationship between city configuration and the canopy UHI effect, the spatial metrics employed by previous studies examining the linkages between urban morphology and other urban climatological processes, such as the surface UHI effect (Liu & Weng, 2008; Connors, Galletti, & Chow, 2013; Schwarz & Manceur, 2014) and air quality (Makido, Dhakal, & Yamagata, 2012; Bereitschaft & Debbage, 2013), were particularly informative. The spatial metrics that were most relevant to our research goals and therefore incorporated into the study included: area-weighted mean patch fractal dimension (AWMPFD), area-weighted mean shape index (AWMSI), clumpiness index (CLUMPY), contagion index (CONTAG), edge density (ED), largest patch index (LPI), patch density (PD), percentage of like adjacencies (PLADJ) and percentage of landscape (PLANL) (Table A.1). Each metric was calculated at the class level (i.e. the metric values were summarized for each individual class present in the landscape) with the exception of CONTAG, which was calculated at the landscape level (i.e. the metric considered all the classes present in landscape simultaneously).

AWMPFD and AWMSI both provide measures of shape complexity based on modified perimeter-area ratios. AWMPFD values vary from 1 (simple shape) to 2 (complex shape) while AWMSI values increase from 1 as the shape becomes more irregular. ED is another metric

commonly used to quantify urban shape complexity, but it is not based on patch perimeter-area ratios. Instead, ED calculates the total length of the urban edge segments, which is then divided by the total landscape area. Within the context of urban landscapes, increasingly irregular and complex shapes typically represent more expansive urban morphologies.

PD and LPI are metrics used to evaluate the fragmentation/aggregation of the urban environment. PD is the number of urban patches divided by the entire landscape area. A larger PD proportion is usually indicative of a more fragmented urban morphology. LPI is of interest when analyzing cities because it quantifies the dominance of the urban core by dividing the area of the largest urban patch, which in most cases would be the Central Business District (CBD) if NLCD Class 24 were being analyzed, by the total landscape area. Lower LPI values are typically associated with increasingly polycentric and fragmented urban environments.

PLADJ, CLUMPY and CONTAG are also measures of fragmentation/aggregation, but they are fundamentally based on adjacency matrices. PLADJ is calculated by dividing the number of like adjacencies involving urban pixels by the total number of adjacencies involving urban pixels. A higher PLADJ indicates a more contiguous urban landscape. CLUMPY builds on the PLADJ metric by comparing the actual proportion of urban like adjacencies to that expected from a spatially random distribution. The values for CLUMPY vary from -1 (maximally disaggregated) to 1 (maximally aggregated) where 0 represents an essentially random distribution. CONTAG is another aggregation metric but it subsumes both interspersion and dispersion by analyzing the entire landscape, not just the urban pixels. CONTAG values range from 0 to 100 with 100 occurring when the landscape is maximally aggregated.

Although described above via an urban-centric perspective, the same suite of spatial metrics was used to evaluate every LULC category. For each city, the eight class level metrics were calculated for all 15 LULC classifications while CONTAG was calculated at the landscape level. If a LULC category was not present within a given MSA, the spatial metrics for that class were assigned to zero.

2.2.3. Control variables

Additional control variables were derived to account for factors previously hypothesized to influence the UHI effect, such as city size, density and climatological conditions (Oke, 1982). City area was defined as the combined area of all the UA/UC included in each MSA. Population density was calculated using 2010 US Census data by summing the populations of the UA/UC within a given MSA and dividing that total population by the derived city area variable.

With regard to the climatological conditions, aridity was estimated using the PRISM datasets for monthly average precipitation and maximum temperature during 2010. Specifically, the monthly average precipitation and maximum temperature for each city were derived by averaging the pixel values within the same UA/UC employed during the UHI estimations. Although fairly simplistic, De Martonne's (1926) aridity index was used (Eq. (2)).

$$I_{AR} = P/(T + 10) \quad (2)$$

In Eq. (2), P is precipitation measured in millimeters and T is temperature measured in degrees Celsius. The index approaches zero as the environment becomes more arid. Annual average aridity was calculated for each city from the individual monthly index values. Since ecological context is largely governed by precipitation and temperature climatology, the aridity variable served as a proxy that accounted for the general character of the various natural environments surrounding the cities. Finally, the monthly and annual average wind speed for each city was calculated using NCEP/NCAR reanalysis data. The reanalysis data were resampled to a 0.10 by 0.10 degree grid to ensure that numerous pixels fell within the UA/UC of each MSA, which again served as the averaging domain.

2.3. Statistical methods

Both bivariate and multivariate statistical techniques were used to evaluate the degree to which city configuration influences UHI intensity. Pearson's correlation coefficient (r) was calculated to analyze the relationships between each of the spatial metrics and the UHI effect. These bivariate relationships were examined for the monthly UHI intensities in 2010, the 2010 annual average UHI intensity and the longer-term average UHI intensity from 2006 to 2010. Comparing the results in 2010 to the longer-term average helped determine if the relationships in 2010 were atypical or fairly consistent with recent history while the monthly analysis enabled an exploration of any seasonality present in the relationships. In addition to evaluating the degree of association between the spatial metrics and UHI intensity, correlation coefficients were also calculated between the UHI effect and each of the control variables.

For the multivariate models, the independent variables that were considered for inclusion encompassed the various components of urban morphology as well as potential confounding factors in order to reduce the likelihood of over-estimating the influence of city configuration on the UHI effect. Specifically, the potential independent variables included all the derived spatial metrics in addition to controls for city area, population density, aridity and wind speed. The independent variables actually incorporated into the multivariate models were manually selected based on a consideration of existing theory, the bivariate correlations and the overarching research goals. The spatial contiguity of low-intensity urban development (PLADJ_22) and the spatial contiguity of high-intensity urban development (PLADJ_24) were included

in each model to evaluate the different influences of sprawling and high-density urban development on the UHI effect. The remaining independent variables, the percentage of barren land (PLAND_31), the shape complexity of deciduous forest (AWMPFD_41), the percentage of shrub land (PLAND_52) and the annual average aridity in 2010 (Aridity), accounted for influential confounding factors. All six independent variables were included in each of the regression models. Several multivariate regression models were estimated to evaluate the relationships at both seasonal and annual timeframes. Specifically, there were six dependent variables of interest: the four 2010 seasonal UHI intensity averages, the 2010 annual average UHI intensity and the 2006 to 2010 annual average UHI intensity.

Despite the advantages of multivariate techniques, namely the ability to analyze the partial effects of multiple variables while controlling for potential confounding factors, Ordinary Least Squares (OLS) regression models are built on a set of assumptions (Hamilton, 1992). Although in actual research these assumptions are seldom, if ever, literally met (Hamilton, 1992), a series of diagnostics can be used to discern the severity of the violations, help evaluate the overall robustness of the results and determine if any corrective measures should be pursued. Firstly, OLS regression fits the best linear relationship between the dependent and independent variables, which is inappropriate if the functional form is fundamentally non-linear. To determine if the relationships between urban morphology and UHI intensities were linear, the functional form of the bivariate scatter plots and the added-variable plots created during the regression analysis were examined.

For the estimated parameters to be unbiased, all relevant independent variables must be included in the model. Determining if all pertinent variables are incorporated is difficult, due to the infinite number of potential independent variables, and typically relies heavily on theoretical justification. Generally, a certain degree of specification bias is unavoidable in regression analysis since all relevant independent variables often cannot be included due to data limitations. To soundly conduct inferential tests on regression model coefficients, the error terms must be: homoskedastic (have constant variance across all values of X), uncorrelated with each other (no autocorrelation) and normally distributed. The error terms of all the models were checked for heteroskedasticity (unequal variance across the values of X) using White's Test (White, 1980), and normalcy was evaluated using histograms. Finally, regression models are sensitive to overly influential observations and multicollinearity (correlation between the independent variables). Overly influential observations were tested for using Cook's D (Cook & Weisberg, 1982) and DFBETAS (Belsley, Kuh, & Welsch, 1980) while the presence of multicollinearity was determined by calculating the correlation coefficients of the independent variables as well as their respective variable inflation factors (VIFs).

3. Results and discussion

3.1. Suitability of PRISM for UHI intensity estimation

On average, roughly 18 stations were considered for the computation of the PRISM grids within each city, with a minimum of approximately 6 and a maximum upwards of 50. The statistically insignificant ($p = 0.66$) correlation between the number of surface observations within each city that were potentially considered by PRISM and the UHI intensity estimates indicates that station availability did not bias the UHI intensity calculations. The ratio calculated between the percentage of urban stations and the percentage of urban land cover had a mean near one (1.14) and a low standard deviation (0.24), implying that the surface observations potentially used in the PRISM interpolation process provided a relatively representative sample of the urban land cover within each city. Importantly, the ratio was insignificantly ($p = 0.33$) correlated with the UHI intensities, which suggests any slight over or under sampling was not substantial enough to systematically bias the UHI estimates.

The insignificant correlations combined with a qualitative visual inspection of the station distributions within each city collectively indicated that PRISM provided an adequately representative depiction of urban temperatures for the cities included in this study. An example of how PRISM successfully resolved the UHI effect of Louisville, Kentucky is provided in Fig. 3. PRISM (Torres-Valcárcel, Harbor, Torres-Valcárcel, & González-Avilés, 2014) and DAYMET (Gallo & Xian, 2014), a similar gridded climate data product, have been used previously to evaluate the UHI effect since they, "potentially provide more

detailed information related to the factors that are relevant to urban heat island analyses" (Gallo & Xian, 2014, p. 9).

3.2. UHI intensities in 2010

In 2010, the minimum temperatures of the fifty cities were on average 0.37 °C warmer than their surrounding natural environments (Fig. 4). Since these are annual average UHI effects, which incorporate both those nights that are optimally and poorly suited for UHI

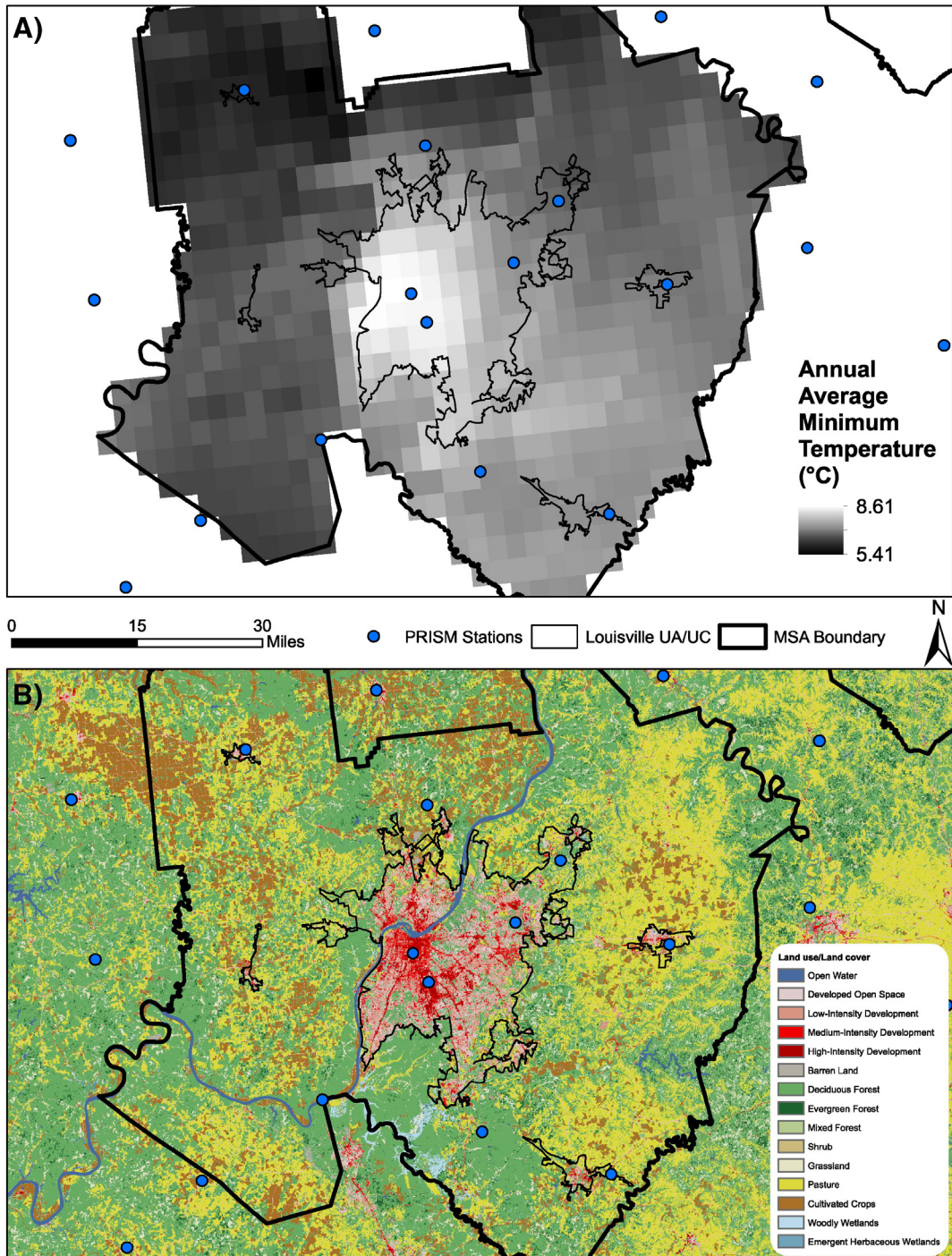


Fig. 3. A) PRISM annual average minimum temperature grid revealing the UHI of Louisville, Kentucky overlaid with the surface observation stations potentially used during the PRISM interpolation process. B) Corresponding NLCD 2006 data for Louisville, Kentucky.

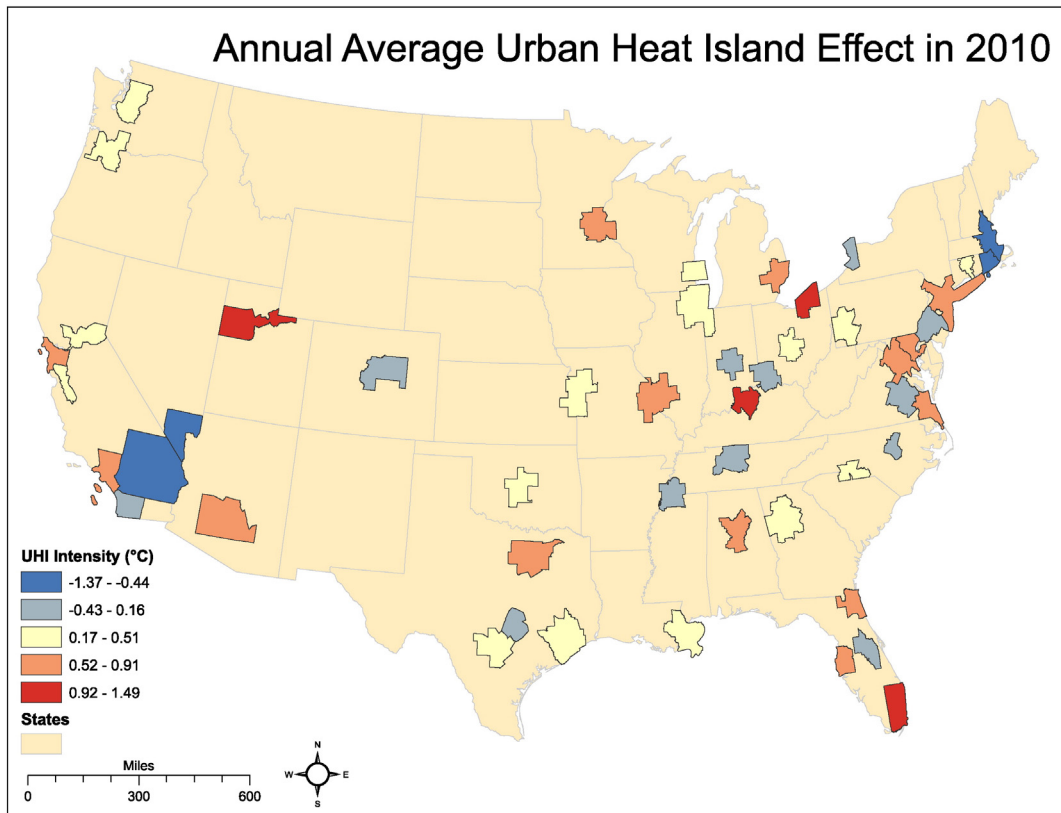


Fig. 4. Map of the annual average UHI intensity ($^{\circ}\text{C}$) in 2010 for the 50 most populous MSAs in the United States.

formation, the magnitudes were never expected to approach the maximum thermal modification under ideal conditions of approximately $12\ ^{\circ}\text{C}$ (Oke, 1987). Averaging the minimum temperatures throughout the entire UA/UC also contributed to the reduced magnitude relative to the potential maximum UHI effect, which is typically obtained by comparing the temperature within the urban core of a city to its rural surroundings. Although minimum temperatures were analyzed in this study, the annual average UHI intensities were more comparable to the $1\text{--}3\ ^{\circ}\text{C}$ amplification of the annual mean air temperature identified by Oke (1997) for large mid-latitude cities.

Salt Lake City exhibited the most intense UHI effect ($1.49\ ^{\circ}\text{C}$), which is partially due to the high prevalence of temperature inversions in that region (Pope et al., 2006) since inversions typically produce calm, clear and stable conditions ideal for UHI formation (Hu et al., 2013). The January peak of the Salt Lake City UHI (Fig. 5) supports this theory since inversions most commonly occur during the colder months (Pope et al., 2006). Salt Lake City has also previously been identified as the most intense UHI amongst numerous American cities (Gallo et al., 1993), although this prior estimate was derived from a weekly instead of annual average and contained less stringent controls for elevation biases. The second most intense UHI of $1.34\ ^{\circ}\text{C}$ occurred in Miami and is potentially attributable to the tall skyscrapers along the coastline creating a wall effect (Wong, Nichol, To, & Wang, 2010), which would impede sea breezes from ventilating the city. Ecological context is also important to consider (Imhoff et al., 2010), as the wetlands surrounding Miami provided a relatively cool rural temperature that contributed to the UHI intensity. The Louisville UHI ($1.12\ ^{\circ}\text{C}$) finalized the top three likely because it was one of very few major American cities without a comprehensive tree ordinance in 2010 (Partnership for a Green City, 2009). The absence of seasonality in the Louisville UHI also suggests that a lack of tree canopy coverage is contributing to the UHI effect since the natural life cycle of vegetation typically enhances seasonal UHI variability (Fig. 5).

In contrast to the intense UHIs of Salt Lake City, Miami and Louisville, the negative values in Fig. 4 indicate that a city was actually cooler than its natural surroundings. Riverside and Las Vegas exhibited the strongest urban cool islands (UCIs) of -1.37 and $-0.76\ ^{\circ}\text{C}$, respectively. This “oasis effect” is largely due to the increased presence of moisture

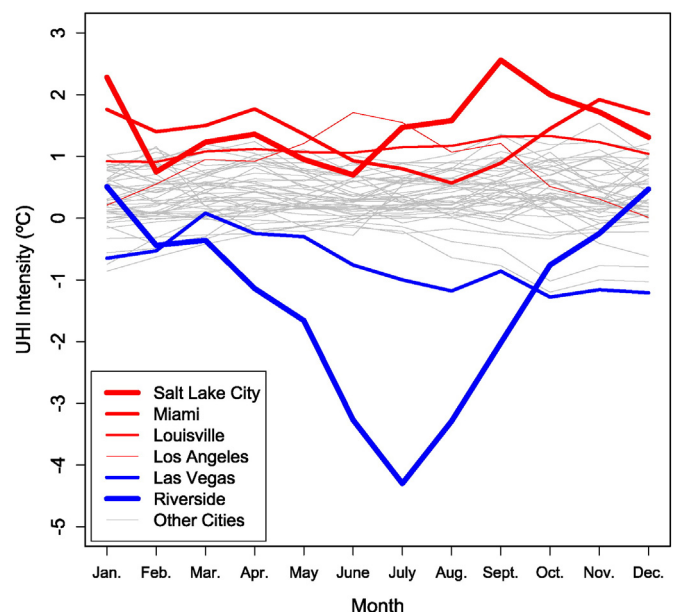


Fig. 5. Monthly UHI Intensities for each MSA in 2010. Gray lines depict values near the consensus while more extreme UHIs and UCIs are highlighted in red and blue, respectively. (For interpretation of the references to color in this figure legend, the reader is referred to the web version of this article.)

and heightened potential for evaporative cooling within the cities relative to the surrounding desert landscapes (Brazel, Selover, Vose, & Heisler, 2000). The Riverside UCI was a particularly extreme case that was partially influenced by the seasonality of aridity (Fig. 5), as the summertime UCI peak occurred during a phase of extremely arid conditions according to the De Martonne index.

Although the lack of comparability between UHI studies that utilize different methodologies prevented a more extensive validation of the UHI intensities, the reasonable magnitudes and the agreement between the reported estimates and mechanisms outlined in the existing literature suggest that the PRISM methodology is suitable for UHI analysis.

Additionally, using a fundamentally areal-based technique to estimate the canopy UHI intensity provides a useful alternative to the traditional urban–rural site comparison approach because it holds the potential to better capture the heterogeneity of temperature within the entire city and its surroundings (Jin, 2012).

3.3. Previously hypothesized factors influencing UHI intensity

While it is somewhat challenging to draw direct comparisons across UHI studies that employ different methodologies, it is still useful to consider the factors previously hypothesized to influence the UHI effect

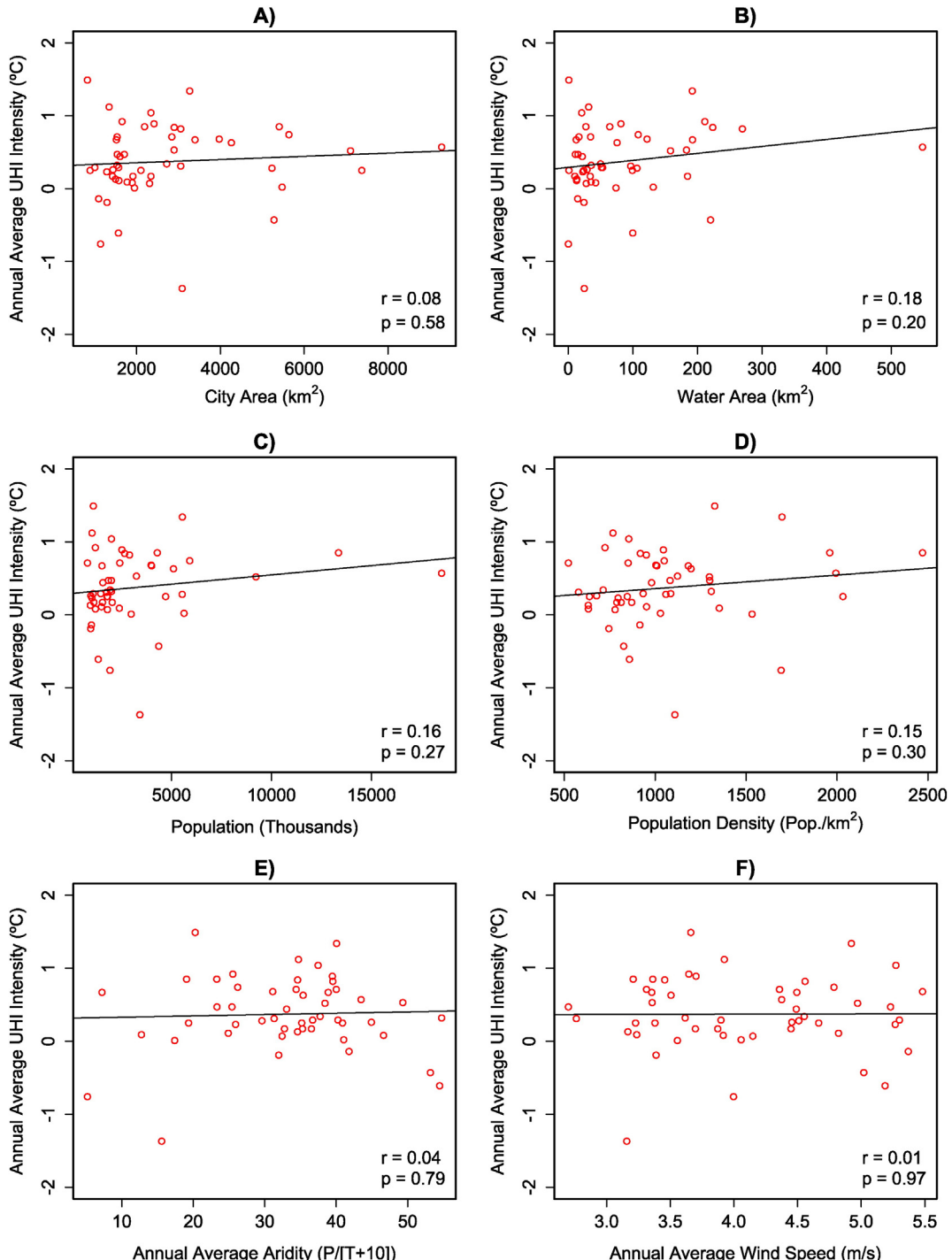


Fig. 6. Relationships between 2010 annual average UHI intensities and previously hypothesized influential factors.

prior to exploring the relationships between UHI intensity and city configuration (Fig. 6). Larger cities in terms of area are thought to produce more intense canopy UHIs (Oke, 1982), although studies focusing on the surface UHI have provided the most empirical evidence for this relationship (Imhoff et al., 2010; Zhou, Rybski, & Kopp, 2013). The annual average canopy UHI intensities of the 50 MSAs were not significantly correlated with city area ($p = 0.58$). This result lends some support to the hypothesis that city area has a minimal influence on UHI intensity and that other factors, which are usually strongly correlated with increases in city area, are actually responsible for this ostensible relationship (Atkinson, 2003). The potential cooling influence of water bodies was also not observed (Park, 1986) since annual average UHI intensity and water area within a city exhibited an insignificant correlation ($p = 0.20$).

Despite the relationship being well documented (Oke, 1973; Park, 1986), there was an insignificant ($p = 0.27$) correlation between UHI intensity and city population. Logarithmic transformations of the population variable were performed but they did not substantially improve the correlations. It appears that the relationship between population size and UHI intensity deteriorates when analyzing exclusively very large cities, since the sample included only the fifty most populous MSAs. The relationship was likely further weakened because the annual average included days where the conditions for UHI formation were not

ideal, unlike the approximate maximum UHI considered by Oke (1973). UHI intensity and population density were also not significantly correlated ($p = 0.30$), which contrasts with previous studies that found population density, rather than total population, to be influential in governing the magnitude of the UHI effect (Steeneveld, Koopmans, Heusinkveld, van Hove, & Holtslag, 2011; Elsayed, 2012; Wolters & Brandsma, 2012). Climatological factors, such as wind speed and aridity, are also known to influence UHI intensities (Oke, 1982), but insignificant relationships were exhibited for the annual averages, with p -values of 0.97 and 0.79, respectively. However, when the monthly UHI intensities in 2010 were compared to the corresponding monthly wind speed and aridity values for each city individually, several significant correlations were discovered.

3.4. City configuration and UHI intensity – bivariate relationships

Of the spatial metrics calculated for the four urban land use classes, the percentage of like adjacencies (PLADJ) had the strongest correlations with UHI intensity. The amount of urban land cover (PLAND) across all four intensity levels was not as strongly correlated with the UHI effect, which indicates that the spatial configuration of urban development, not merely its abundance, is of importance. The PLADJ for developed open space (PLADJ_21), low-intensity development

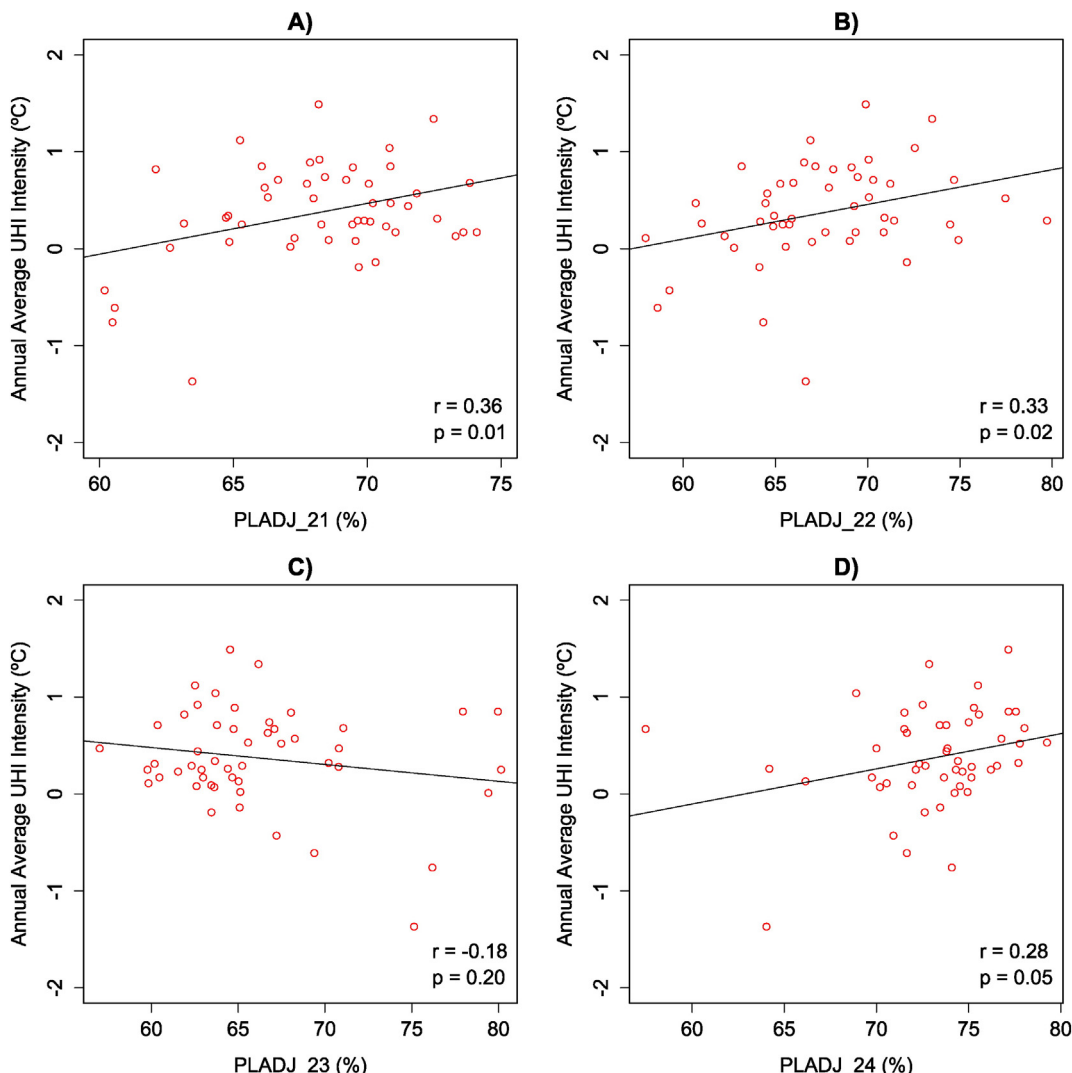


Fig. 7. Correlations between annual average UHI intensity in 2010 and the percentage of like adjacencies (PLADJ) for developed open space (21), low-intensity development (22), medium-intensity development (23) and high-intensity development (24).

(PLADJ_22) and high-intensity development (PLADJ_24) all had significant ($p < 0.05$) positive correlations with UHI intensity (Fig. 7). Therefore, increasing the spatial contiguity of urban development across a wide spectrum of intensity levels appears to enhance the UHI effect amongst large US cities. One caveat was the contiguity of medium-intensity development (PLADJ_23), which did not have a positive correlation with UHI intensity. The correlation coefficient was negative, albeit insignificant ($p = 0.20$), in part because the arid cities of the Southwest, particularly Riverside and Las Vegas, were characterized by strong UCIs and high PLADJ_23 values. When Riverside and Las Vegas were omitted, the correlation coefficient was positive but still not significantly different from zero ($p = 0.84$), which makes it challenging to draw any robust conclusions.

Finding that UHIs are generally magnified by more contiguous urban development, across a variety of urban intensity levels, potentially elucidates the false dichotomy implied by previous research that either sprawling (Stone & Rodgers, 2001; Stone, 2012) or high-density (Coutts et al., 2007; Martilli, 2014) city configurations amplify UHI intensities. Instead, our results suggest that sprawling and high-density city configurations both have the propensity to increase UHI intensities if the urban development is highly contiguous.

The correlations between the spatial contiguity of urban development and UHI intensity varied throughout the year due to the seasonality of the UHI effect (Table 1). The relationships exhibited clear seasonal trends, as the PLADJ for high-intensity urban development (PLADJ_24) was most strongly correlated with UHI intensity during the summer months of June, July and August. The spatial contiguity of developed open space (PLADJ_21) and low-intensity development (PLADJ_22), in contrast, displayed stronger relationships with UHI intensity during the late fall and winter. Finally, the contiguity of medium-intensity urban development (PLADJ_23) was again an exception since it was insignificantly ($p > 0.05$) correlated with UHI intensity throughout the year.

The bottom portion of Table 1 compared the relationships between urban spatial contiguity and the annual average UHI intensity in 2010 with the correlations estimated for the longer-term 2006 to 2010 annual average UHI intensity. Relative to the 2010 correlation coefficients, the contiguity of high-intensity urban development (PLADJ_24) had a marginally stronger relationship with UHI intensity when analyzing the longer-term annual average whereas the correlations for the contiguity of low-intensity development (PLADJ_22) and developed open space (PLADJ_21) were marginally weaker. However, the overall differences between the correlation coefficients for the 2010 annual average and the longer-term average were minimal, suggesting that

the relationships between urban spatial contiguity and UHI intensity observed in 2010 were fairly typical and consistent with recent history.

3.5. City configuration and UHI intensity – multivariate models

OLS regression models were used to further disentangle the influences of sprawling and high-density urban development on UHI intensities. The original no-omission regression model, which included all the cities, violated the diagnostic tests for Cook's D and DFBETAS, indicating that the sample included extreme and overly influential values (Table S1). The no-omission model also suffered from heteroskedasticity as it failed to meet the criteria of White's Test, which can partially be attributed to the difficulty of predicting the extreme values. In order to better meet the assumptions of multivariate regression modeling, the overly influential cities were omitted from the remaining models. Firstly, Miami and Tampa were omitted because they did not contain any deciduous forest, which meant their respective values for AWMPFD_41 were assigned to zero and therefore fairly extreme. Secondly, Las Vegas, Phoenix and Riverside were omitted because the lack of other arid cities within the sample made them overly influential, particularly during the summer.

Excluding the five cities mentioned above from the remaining regression models provided much more robust estimates, as indicated by the model diagnostics. Overly influential observations were not present, as Cook's D never exceeded 0.32 (Cook's D values greater than 1 are considered to be overly influential). Multicollinearity was also minimal since the VIFs were less than 1.6 (VIFs greater than 4 are typically indicative of problematic levels of multicollinearity). Finally, heteroskedasticity was negligible as the p-values for White's Test were never below 0.07 (p-values less 0.05 would result in a rejection of the null hypothesis of homoskedasticity). A full output table is only provided for the model estimated with the 2010 annual average UHI intensity as the dependent variable, but complete details for the no-omission (Table S1), long-term average (Table S2) and seasonal (Tables S3–S6) models are all provided in the supplementary information.

Overall, the model performed well when analyzing the 2010 annual average, as it explained almost half of the variability in UHI intensity (Table 2). There was very little reduction in the adjusted R-Squared value, which suggests that the model was not overly complex. The partial slope coefficients indicated that the spatial contiguity of high-intensity urban development (PLADJ_24) had a statistically significant ($p < 0.05$) relationship with UHI intensity. Specifically, a ten percentage point increase in the spatial contiguity of high-intensity urban development, the equivalent of shifting roughly from Orlando (PLADJ_24 = 69.8%) to Seattle (PLADJ_24 = 79.3%), was predicted to enhance a city's annual average UHI intensity by 0.4 °C. This is quite a substantial UHI amplification, especially considering that the annual average UHI effects had a fairly modest mean value of 0.37 °C. The partial slope coefficient for the spatial contiguity of low-intensity urban development (PLADJ_22) was also significant, as a ten percentage point increase was predicted to enhance a city's annual average UHI intensity by 0.3 °C. Therefore, as suggested by the bivariate analysis, both low and high-density urban land uses appear to amplify the UHI effect if they are highly contiguous.

The remaining variables included in the model accounted for the influences of non-urban land covers and aridity on the annual average UHI intensity. The partial slope coefficient for the proportion of barren land (PLAND_31) was significant and positive, as the overall dearth of vegetation present within the barren class was likely partially responsible for increased UHI intensities. However, the heterogeneity of the LULCs included in the NLCD barren category complicates this interpretation slightly. Deciduous forest shape complexity (AWMPFD_41) also had a significant influence on UHI intensity, as increasingly complex forest shapes were predicted to enhance the UHI effect. Since increased deciduous forest shape complexity is likely due to the fragmentation

Table 1

Correlation coefficients between the average UHI intensity for various time periods and the PLADJ metrics for each urban intensity level.

Time period	PLADJ_21	PLADJ_22	PLADJ_23	PLADJ_24
January average	0.34*	0.43**	-0.23	0.06
February average	0.35*	0.40**	-0.13	0.22
March average	0.22	0.23	0.03	0.21
April average	0.28-	0.22	-0.13	0.20
May average	0.24-	0.11	-0.07	0.20
June average	0.23	0.09	-0.16	0.33*
July average	0.22	0.17	-0.19	0.42**
August average	0.32*	0.22	-0.19	0.43**
September average	0.29*	0.23	-0.07	0.32*
October average	0.40**	0.45**	-0.23	0.25-
November average	0.42**	0.44**	-0.23	0.12
December average	0.46***	0.43**	-0.24-	-0.02
2010 annual average	0.36**	0.33*	-0.18	0.28*
2006–2010 annual average	0.36*	0.32*	-0.15	0.30*

- Sig. level $p < 0.10$.

* Sig. level $p < 0.05$.

** Sig. level $p < 0.01$.

*** Sig. level $p \sim 0.000$.

Table 2

2010 annual average regression model. Annual average UHI intensity in 2010 is the dependent variable. The anomalous cities of Miami, Tampa, Phoenix, Las Vegas and Riverside were omitted ($N = 45$).

Independent variable	Coefficient	Std. coefficient	p-Value	Sig. level
Constant	-9.857		0.00	***
PLADJ_22	0.028	0.33	0.02	*
PLADJ_24	0.039	0.30	0.03	*
PLAND_31	0.380	0.28	0.03	*
AWMPFD_41	5.161	0.42	0.00	**
PLANL_52	-0.028	-0.16	0.28	
Aridity	-0.020	-0.49	0.00	**
R-Squared	0.46			
Adjusted R-Squared	0.38			
F-statistic	5.46		0.00	***

Sig. levels: - = $p < 0.10$; * = $p < 0.05$; ** = $p < 0.01$; *** = $p \sim 0.000$.

caused by urban expansion, it is logical that more complexly shaped forests were indicative of more intense UHIs. Unlike barren land and forest shape complexity, the presence of vegetative shrub land (PLANL_52) actually had a mitigating effect on UHI intensities, albeit insignificant ($p > 0.10$). Finally, the model predicted that cities located in relatively more arid environments would have stronger UHIs, but this was perhaps due to the omission of the overly influential arid cities.

To summarize the seasonality of the relationships, the regression coefficients for the contiguity of low-intensity (PLADJ_22) and high-intensity urban development (PLADJ_24) in the models estimated with the seasonal average UHI intensities as dependent variables were graphed by vertical bars in the left panel of Fig. 8. During the winter, the overall predictive power of the model was comparable to the results for the annual average as its R-Squared value was 0.47 (Table S3). The spatial contiguity of high-intensity urban development (PLADJ_24) was less influential in governing UHI intensities during the winter. However, the partial slope coefficient for the spatial contiguity of low-intensity urban development (PLADJ_22) was highly significant ($p < 0.01$), as a ten percentage point increase was predicted to enhance the winter UHI effect by almost 0.4 °C. The model performed

poorest during the spring since it explained roughly one third of the variability in the average spring UHI intensity (Table S4). The spatial contiguity of low-intensity urban development did not significantly ($p = 0.39$) influence the spring UHI effect while the spatial contiguity of high-intensity urban development (PLADJ_24) had only a marginally significant ($p = 0.09$) partial effect. However, the magnitude of this partial slope coefficient was still relevant, as a ten percentage point increase in the contiguity of high-intensity development was predicted to enhance the spring UHI effect by roughly 0.3 °C. With regard to the summer months, the model explained just over 45% of the variability in the average summer UHI intensity (Table S5). The spatial contiguity of high-intensity urban development (PLADJ_24) was significant ($p < 0.05$) during the summer whereas the spatial contiguity of low-intensity urban development (PLADJ_22) was of only marginal significance ($p = 0.10$). Finally, the partial slope coefficients for the spatial contiguity of low and high-intensity urban development were both significant ($p < 0.05$) during the fall, as the model explained almost half of the variability in the average fall UHI intensity (Table S6). A ten percentage point increase in the spatial contiguity of either low or high-intensity urban development was predicted to enhance the fall UHI effect by slightly more than 0.4 °C.

The right panel of Fig. 8 compared the regression coefficients for the spatial contiguity of high (PLADJ_24) and low-intensity (PLADJ_22) urban development when the longer-term annual average UHI intensity was the dependent variable with the results from 2010. This helped ensure that the relationships between city contiguity and the UHI effect observed in 2010 were not anomalous. When analyzing the longer-term annual average, the model explained roughly half of the variability in UHI intensity (Table S2). The spatial contiguity of high-intensity urban development (PLADJ_24) had a significant ($p < 0.05$) influence on both the 2006 to 2010 and 2010 average UHI effects but exhibited a slightly larger magnitude when analyzing the longer-term average (0.043 versus 0.039). The partial slope coefficient for the spatial contiguity of low-intensity urban development (PLADJ_21), in contrast, was only marginally significant ($p = 0.05$) and exhibited a slightly reduced magnitude (0.024 versus 0.028) when the longer-term average was the dependent variable. However, the general similarities suggest that the relationships in 2010 were fairly consistent with recent history.

Although the nature of the data, particularly the commonality of extreme outliers, created modeling difficulties and resulted in the omission of five cities from the majority of the analysis, the regression models collectively provided a compelling diagnosis of the UHI effect. The results suggest that more contiguous urban development across a spectrum of intensity levels can amplify the annual average and seasonal average UHI effects (Fig. 8). This partially reconciles the false dichotomy implied by previous research that either sprawling (Stone & Rodgers, 2001; Stone, 2012) or high-density (Coutts et al., 2007; Martilli, 2014) city configurations enhance the UHI effect. Instead, at least amongst large American cities, both sprawling and high-density configurations appear to magnify UHI intensities if the urban development is highly contiguous. Increasing the spatial contiguity of low or high-intensity urban development ten percentage points was predicted to enhance the UHI effect by a minimum of 0.1 °C in the spring and a maximum of almost 0.5 °C in the fall (Fig. 8). Additionally, during the summer when the overly influential cities were not omitted from the model, the UHI amplification resulting from a ten percentage point increase in the spatial contiguity of high-intensity urban development reached almost 1 °C. Therefore, the results presented in Table 2 and Tables S2–S6 provide inherently conservative estimates of how urban spatial contiguity influences UHI intensities.

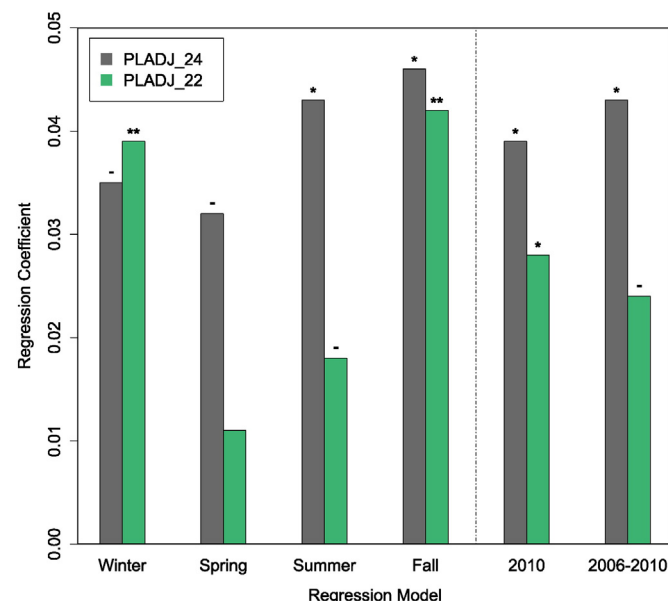


Fig. 8. The vertical bars represent the regression coefficients for the spatial contiguity of low (PLADJ_22) and high-intensity (PLADJ_24) urban development. The left panel displays the coefficients from the seasonal models (Tables S3–S6) while the right panel displays the coefficients for the 2010 annual average model (Table 2) and the longer-term 2006–2010 annual average model (Table S2). Sig. levels: - = $p > 0.10$; * = $p < 0.05$; ** = $p < 0.01$; *** = $p \sim 0.000$.

4. Urban planning implications and conclusions

By developing a methodology to estimate UHI intensities from PRISM climate data and utilizing spatial metrics to quantify urban morphology, this study has found that the spatial contiguity of urban

development makes a statistically significant contribution to the UHI effect. The shape complexity, polycentrism and relative abundance of urban development were all less influential, which emphasizes the potential for contiguous, uninterrupted urban footprints to enhance urban temperatures. An ulterior motive of this research was to examine the urban planning implications of this central finding and potentially clarify if increasing urban densities is a viable UHI mitigation strategy. Based on the correlations and multiple regression models, more contiguous urban development across a range of intensity levels magnifies the UHI effect. Therefore, simply increasing urban densities, which would presumably also increase the contiguity of high-intensity urban development (PLADJ_24), is not likely a viable UHI mitigation strategy. Additionally, policies encouraging infill development also appear potentially detrimental from an UHI perspective since they would increase city contiguity further.

Advocating for urban densification as a UHI mitigation plan is particularly troubling given the seasonality exhibited by the correlations (Table 1) and regression coefficients (Fig. 8). Increasing the contiguity of high-intensity urban development was predicted to enhance UHI intensities most significantly during the summer and fall months, which is precisely when cities are most vulnerable to heat waves. At the opposite end of the urban development intensity spectrum, increasing the contiguity of low-intensity urban development and developed open space also magnified the UHI effect. However, since these relationships were strongest during the winter months, highly contiguous low-intensity urban development and developed open space could potentially be beneficial by reducing the amount of energy used to heat buildings.

Interpreting the statistical models very literally, any city configuration that reduces the contiguity of urban development would potentially mitigate the UHI effect. However, in reality certain LULC types would more successfully accomplish this goal. The inclusion of urban green spaces and parks would decrease the contiguity of urban development and simultaneously provide an additional cooling influence via evapotranspiration. If the total green space area were held constant, interspersing several smaller green spaces throughout the urban fabric would provide a more substantial reduction in urban contiguity than a singular park of greater size. Therefore, networks of smaller urban green spaces seem to hold considerable potential for UHI mitigation. While increasing urban densities alone appears somewhat problematic, UHI intensities may be more successfully alleviated if densification was accompanied by networks of smaller urban parks that would substantially reduce the contiguity of high-intensity urban development. Additionally, white and green roof mitigation techniques could be incorporated in such a scenario since they become more economically feasible at higher density levels (Stone, 2012).

Overall, planning to reduce UHI intensities is very complex and the policies will likely need to be tailored to individual cities. This is partic-

ularly true given that the seasonality of the UHI effect, an important component when evaluating the benefits of a warmer winter versus the detriments of a warmer summer, was very localized to each city (Fig. 5). Additionally, policies have to comprehensively address the entire urban system and not simply focus on the UHI effect in isolation. While high urban densities have traditionally been considered detrimental from an urban climatological perspective (Oke, 1982; Coutts et al., 2001), they can provide benefits, such as improving air quality, increasing the feasibility for public transit, decreasing energy consumption and promoting more active lifestyles, when compared to more sprawling morphologies (Ewing, Pendall, & Chen, 2002). Therefore, the success of any UHI mitigation strategy hinges largely on its ability to reduce the temperatures observed within cities without disrupting the complex array of feedbacks associated with the greater urban metabolism (Kennedy, Cuddihy, & Engel-Yan, 2007). When the urban system is considered in its entirety, discontiguous high-intensity urban development may emerge as a useful compromise since such a configuration would likely preserve the broader benefits of higher densities while simultaneously moderating UHI intensity. The historic downtown district of Savannah, Georgia provides a more concrete example of the rather abstract discontiguous high-intensity city configuration concept, as its network of over twenty heavily vegetated squares reduces the contiguity of the high-intensity urban development substantially.

Admittedly, future work will be needed to help further elucidate the influence of city contiguity on the UHI effect and more fully evaluate the potential of discontiguous high-intensity urban development as a viable UHI mitigation strategy. Since this study was based on statistical modeling, one promising avenue for future research is the usage of physically-based models to analyze how city contiguity impacts specific components of the urban energy balance. Physically-based modeling approaches, which more explicitly account for the three dimensionality of the urban environment, may also be able to further clarify the caveat discovered for medium-intensity development.

The results also must be generalized with caution since the study focuses solely on large American cities. Future research will analyze if and how the relationships between city configuration and UHI intensity vary for cities of different sizes and for those located in other portions of the world. Despite these qualifications, the current findings demonstrate that the spatial contiguity of urban development is an important and previously unidentified contributing factor to the UHI effect, which deserves consideration when devising strategies for UHI mitigation.

Acknowledgments

We would like to thank the three anonymous reviewers and J. A. Knox for providing constructive feedback on the manuscript.

Appendix A

Table A.1

Equations and descriptions of the spatial metrics used to quantify the urban morphologies of the MSAs. Adapted from McGarigal et al. (2012).

Spatial metric	Equation	Description
Area-weighted mean patch fractal dimension (AWMPFD)	$\text{AWMPFD} = \sum_{j=1}^n \left[\left(\frac{2 \ln(0.25p_{ij})}{\ln a_{ij}} \right) \left(\frac{a_{ij}}{\sum_{j=1}^n a_{ij}} \right) \right]$	Where p_{ij} is the perimeter of patch ij and a_{ij} is the area of patch ij (i = number of patch types, j = number of patches)
Area-weighted mean shape index (AWMSI)	$\text{AWMSI} = \sum_{j=1}^n \left[\left(\frac{0.25p_{ij}}{\sqrt{a_{ij}}} \right) \left(\frac{a_{ij}}{\sum_{j=1}^n a_{ij}} \right) \right]$	Where p_{ij} is the perimeter of patch ij and a_{ij} is the area of patch ij (i = number of patch types, j = number of patches)
Clumpiness index (CLUMPY)	Given $G_i = \left(\frac{g_{ii}}{\sum_{k=1}^m g_{ik}} \right)$ $\text{CLUMPY} = \begin{cases} \frac{G_i - P_i}{1 - P_i} & \text{for } G_i \geq P_i \\ \frac{G_i - P_i}{1 - P_i} & \text{for } G_i < P_i \& P_i \geq 0.5 \\ \frac{P_i - G_i}{1 - P_i} & \text{for } G_i < P_i \& P_i < 0.5 \end{cases}$	Where g_{ij} is the number of like adjacencies between pixels of patch type i based on the double count method, g_{ik} is the number of adjacencies between pixels of patch types i and k based on the double-count method, and P_i is the proportion of the landscape occupied by patch type i

Table A.1 (continued)

Spatial metric	Equation	Description
Contagion Index (CONTAG)	$\text{CONTAG} = \left[1 + \frac{\sum_{i=1}^m \sum_{k=1}^m \left[(P_i) \left(\frac{g_{ik}}{\sum_{k=1}^m g_{ik}} \right) \right] * \left[\ln(P_i) \left(\frac{g_{ik}}{\sum_{k=1}^m g_{ik}} \right) \right]}{2 \ln(m)} \right] * 100$	Where P_i is the proportion of the landscape occupied by patch type i, g_{ik} is the number of adjacencies between pixels of patch types i and k based on the double-count method, and m is the number of patch types present in the landscape
Edge density (ED)	$\text{ED} = \frac{\sum_{k=1}^m e_{ik}}{A} * 10,000$	Where e_{ik} is the total edge length (m) of class i in the landscape and A is the total landscape area; the result is multiplied by 10,000 to convert to hectares
Largest patch index (LPI)	$\text{LPI} = \frac{\max_{j=1}^n (a_{ij})}{A} * 100$	Where $\max (a_{ij})$ is the area (m^2) of the largest patch of the corresponding class and A is the total landscape area (m^2); the result is multiplied by 100 to convert to a percentage
Patch density (PD)	$\text{PD} = \frac{n_i}{A} * 10,000 * 100$	Where n_i is the number of patches in the landscape of patch type i and A is the total landscape area (m^2)
Percentage of like adjacencies (PLADJ)	$\text{PLADJ} = \left(\frac{g_{ii}}{\sum_{k=1}^m g_{ik}} \right) * 100$	Where g_{ii} is the number of like adjacencies between pixels of patch type i and g_{ik} is the number of adjacencies between pixels of patch types i and k
Percentage of landscape (PLAN)	$\text{PLAN} = \frac{\sum_{j=1}^n a_{ij}}{A} * 100$	Where a_{ij} is the area (m^2) of patch ij and A is the total landscape area (m^2); the result is multiplied by 100 to convert to a percentage

Appendix B. Supplementary data

Supplementary data to this article can be found online at <http://dx.doi.org/10.1016/j.compenvurbsys.2015.08.002>.

References

- Arnfield, A. J. (2003). Two decades of urban climate research: A review of turbulence, exchanges of energy and water, and the urban heat island. *International Journal of Climatology*, 23(1), 1–26.
- Atkinson, B. W. (2003). Numerical modeling of urban heat-island intensity. *Boundary-Layer Meteorology*, 109(3), 285–310.
- Belsley, D. A., Kuh, E., & Welsch, R. E. (1980). *Regression diagnostics: Identifying influential data and sources of collinearity*. New York: Wiley.
- Bereitschaft, B., & Debbage, K. (2013). Urban form, air pollution, and CO₂ emissions in large U.S. metropolitan areas. *Professional Geographer*, 65(4), 612–635.
- Bereitschaft, B., & Debbage, K. (2014). Regional variations in urban fragmentation among U.S. metropolitan and megapolitan areas. *Applied Spatial Analysis and Policy*, 7(2), 119–147.
- Brazel, A., Selover, N., Vose, R., & Heisler, G. (2000). The tale of two climates – Baltimore and Phoenix urban LTER sites. *Climate Research*, 15(2), 123–135.
- Burchell, R. W., Downs, A., Seskin, S., Moore, T., Listokin, D., ... Phillips, H. (1998). *The cost of sprawl revisited: The evidence of sprawl's negative and positive impacts*. Washington, D.C.: Transportation Research Board.
- Cardelino, C. A., & Chameides, W. L. (1990). Natural hydrocarbons, urbanization, and urban ozone. *Journal of Geophysical Research: Atmospheres*, 95(D9), 13971–13979.
- Connors, J. P., Galletti, C. S., & Chow, W. T. L. (2013). Landscape configuration and urban heat island effects: Assessing the relationship between landscape characteristics and land surface temperature in Phoenix, Arizona. *Landscape Ecology*, 28(2), 271–283.
- Cook, R. D., & Weisberg, S. (1982). *Residuals and influence in regression*. New York: Chapman and Hall.
- Coutts, A. M., Beringer, J., & Tapper, N. J. (2007). Impact of increasing urban density on local climate: Spatial and temporal variations in the surface energy balance in Melbourne, Australia. *Journal of Applied Meteorology and Climatology*, 46(4), 477–493.
- Daly, C., Halbleib, M., Smith, J. I., Gibson, W. P., Doggett, M. K., ... Pasteris, P. P. (2008). Physiographically sensitive mapping of climatological temperature and precipitation across the conterminous United States. *International Journal of Climatology*, 28(15), 2031–2064.
- De Martonne, E. (1926). Une nouvelle fonction climatologique: L'indice d'aridité. *La Météorologie*, 2, 449–458.
- Elsayed, I. S. M. (2012). Effects of population density and land management on the intensity of urban heat islands: A case study on the city of Kuala Lumpur, Malaysia. In B. M. Alam (Ed.), *Application of geographic information systems* (pp. 267–282). Rijeka, Croatia: Intech.
- Emmanuel, R., & Fernando, H. J. S. (2007). Urban heat islands in humid and arid climates: Role of urban form and thermal properties in Colombo, Sri Lanka and Phoenix, USA. *Climate Research*, 34(3), 241–251.
- Ewing, R., & Rong, F. (2008). The impact of urban form on U.S. residential energy use. *Housing Policy Debate*, 19(1), 1–30.
- Ewing, R., Pendall, R., & Chen, D. (2002). *Measuring sprawl and its impact*. Washington, D.C.: Smart Growth America (<<http://www.smartgrowthamerica.org/documents/MeasuringSprawl.PDF>>).
- Fry, J. A., Xian, G., Jin, S., Dewitz, J. A., Homer, C. G., ... Wickham, J. D. (2011). Completion of the 2006 national land cover database for the conterminous United States. *Photogrammetric Engineering & Remote Sensing*, 77(9), 858–864.
- Gallo, K., & Xian, G. (2014). Application of spatially gridded temperature and land cover data sets for urban heat island analysis. *Urban Climate*, 8, 1–10.
- Gallo, K. P., McNab, A. L., Karl, T. R., Brown, J. F., Hood, J. J., & Tarpley, J. D. (1993). The use of NOAA AVHRR data for assessment of the urban heat island effect. *Journal of Applied Meteorology*, 32(5), 899–908.
- Galster, G., Hanson, R., Ratcliffe, M. R., Wolman, H., Coleman, S., & Freihage, J. (2001). Wrestling sprawl to the ground: Defining and measuring an elusive concept. *Housing Policy Debate*, 12(4), 681–717.
- Haeger-Eugensson, M., & Holmer, B. (1999). Advection caused by the urban heat island circulation as a regulating factor on the nocturnal urban heat island. *International Journal of Climatology*, 19(9), 975–988.
- Hamilton, L. C. (1992). *Regression with graphics: A second course in applied statistics*. Pacific Grove, CA: Brooks/Cole.
- Herold, M., Couclelis, H., & Clarke, K. C. (2005). The role of spatial metrics in the analysis and modeling of urban land use change. *Computers, Environment and Urban Systems*, 29(4), 369–399.
- Herold, M., Goldstein, N. C., & Clarke, K. C. (2003). The spatiotemporal form of urban growth: Measurement, analysis and modeling. *Remote Sensing of Environment*, 86(3), 286–302.
- Herold, M., Scepan, J., & Clarke, K. C. (2002). The use of remote sensing and landscape metrics to describe structures and changes in urban land uses. *Environment and Planning A*, 34(8), 1443–1458.
- Herold, M., Goldstein, N. C., & Clarke, K. C. (2003). The spatiotemporal form of urban growth: Measurement, analysis and modeling. *Remote Sensing of Environment*, 86(3), 286–302.
- Hu, X. M., Klein, P. M., Xue, M., Lundquist, J. K., Zhang, F., & Qi, Y. (2013). Impact of low-level jets on the nocturnal urban heat island intensity in Oklahoma City. *Journal of Applied Meteorology and Climatology*, 52(8), 1779–1802.
- Huang, J., Lu, X. X., & Sellers, J. M. (2007). A global comparative analysis of urban form: Applying spatial metrics and remote sensing. *Landscape and Urban Planning*, 82(4), 184–197.
- Imhoff, M. L., Zhang, P., Wolfe, R. E., & Bounoua, L. (2010). Remote sensing of the urban heat island effect across biomes in the continental USA. *Remote Sensing of Environment*, 114(3), 504–513.
- Jat, M. K., Garg, P. K., & Khare, D. (2008). Monitoring and modeling of urban sprawl using remote sensing and GIS techniques. *International Journal of Applied Earth Observation and Geoinformation*, 10(1), 26–43.
- Ji, W., Ma, J., Twibell, R. W., & Underhill, K. (2006). Characterizing urban sprawl using multi-stage remote sensing images and landscape metrics. *Computers, Environment and Urban Systems*, 30(6), 861–879.
- Jin, M. S. (2012). Developing an index to measure urban heat island effect using satellite land skin temperature and land cover observations. *Journal of Climate*, 25(18), 6193–6201.
- Johnson, D. P., & Wilson, J. S. (2009). The socio-spatial dynamics of extreme urban heat events: The case of heat-related deaths in Philadelphia. *Applied Geography*, 29(3), 419–434.
- Kennedy, C., Cuddihy, J., & Engel-Yan, J. (2007). The changing metabolism of cities. *Journal of Industrial Ecology*, 11(2), 43–59.
- Li, D., & Bou-Zeid, E. (2013). Synergistic interactions between urban heat islands and heat waves: The impact in cities is larger than the sum of its parts. *Journal of Applied Meteorology and Climatology*, 52(9), 2051–2064.

- Liu, H., & Weng, Q. (2008). Seasonal variations in the relationship between landscape pattern and land surface temperature in Indianapolis, USA. *Environmental Monitoring and Assessment*, 144, 199–219.
- Makido, Y., Dhakal, S., & Yamagata, Y. (2012). Relationship between urban form and CO₂ emissions: Evidence from fifty Japanese cities. *Urban Climate*, 2, 55–67.
- Martilli, A. (2014). An idealized study of city structure, urban climate, energy consumption, and air quality. *Urban Climate*, 10(2), 430–446.
- McGarigal, K., Cushman, S. A., & Ene, E. (2012). FRAGSTATS v4: Spatial pattern analysis program for categorical and continuous maps. Amherst: University of Massachusetts (<<http://www.umass.edu/landeco/research/fragstats/fragstats.html>>).
- McMichael, A. J., Woodruff, R. E., & Hales, S. (2006). Climate change and human health: Present and future risks. *The Lancet*, 367(9513), 859–869.
- Oke, T. R. (1973). City size and the urban heat island. *Atmospheric Environment*, 7(8), 769–779.
- Oke, T. R. (1982). The energetic basis of the urban heat island. *Quarterly Journal of the Royal Meteorological Society*, 108(455), 1–24.
- Oke, T. R. (1987). *Boundary layer climates*. New York: Methuen.
- Oke, T. R. (1997). Urban climates and global environmental change. In R. D. Thompson, & A. Perry (Eds.), *Applied climatology: Principles & practices* (pp. 273–287). New York: Routledge.
- Oke, T. R., & East, C. (1971). The urban boundary layer in Montreal. *Boundary-Layer Meteorology*, 1(4), 411–437.
- Park, H. S. (1986). Features of the heat island in Seoul and its surrounding cities. *Atmospheric Environment*, 20(10), 1859–1866.
- Partnership for a Green City (2009). *Climate action report*. (<<http://www.jeffersonkyschools.us/projects/greenicity/ClimateActionRpt.pdf>>).
- Patz, J. A., Campbell-Lendrum, D., Holloway, T., & Foley, J. A. (2005). Impact of regional climate change on human health. *Nature*, 438(7066), 310–317.
- Peng, S., Piao, S., Ciais, P., Friedlingstein, P., Ottle, C., ... Myneni, R. B. (2011). Surface urban heat island across 419 global big cities. *Environmental Science & Technology*, 46(2), 696–703.
- Pope, C. A., Muhlestein, J. B., May, H. T., Renlund, D. G., Anderson, J. L., & Horne, B. D. (2006). Ischemic heart disease events triggered by short-term exposure to fine particulate air pollution. *Circulation*, 114(23), 2443–2448.
- Population Reference Bureau (2013). 2013 World population datasheet. (<http://www.prb.org/pdf13/2013-population-data-sheet_eng.pdf>).
- Rosenfeld, A. H., Akbari, H., Romm, J. J., & Pomerantz, M. (1998). Cool communities: Strategies for heat island mitigation and smog reduction. *Energy and Buildings*, 28(1), 51–62.
- Sarrat, C., Lemonsu, A., Masson, V., & Guedalia, D. (2006). Impact of urban heat island on regional atmospheric pollution. *Atmospheric Environment*, 40(10), 1743–1758.
- Schwarz, N., & Manceur, A. M. (2014). Analyzing the influence of urban forms on surface urban heat islands in Europe. *Journal of Urban Planning and Development* <[http://dx.doi.org/10.1061/\(ASCE\)UP.1943-5444.0000263](http://dx.doi.org/10.1061/(ASCE)UP.1943-5444.0000263)>.
- Souch, C., & Grimmond, S. (2006). Applied climatology: Urban climate. *Progress in Physical Geography*, 30(2), 270–279.
- Steenneveld, G. J., Koopmans, S., Heusinkveld, B. G., van Hove, L. W. A., & Holtslag, A. A. M. (2011). Quantifying urban heat island effects and human comfort for cities of variable size and urban morphology in Netherlands. *Journal of Geophysical Research: Atmospheres*, 116(D20) <<http://dx.doi.org/10.1029/2011JD015988>>.
- Stewart, I. D. (2011). A systematic review and scientific critique of methodology in modern urban heat island literature. *International Journal of Climatology*, 31(2), 200–217.
- Stone, B. (2012). *The city and the coming climate: Climate change in the places we live*. New York: Cambridge University Press.
- Stone, B., & Rodgers, M. O. (2001). Urban form and thermal efficiency: How the design of cities influences the urban heat island effect. *Journal of the American Planning Association*, 67(2), 186–198.
- Stone, B., Hess, J. J., & Frumkin, H. (2010). Urban form and extreme heat events: Are sprawling cities more vulnerable to climate change than compact cities? *Environmental Health Perspectives*, 118(10), 1425–1428.
- Sutton, P. C., Goetz, A. R., Fildes, S., Forster, C., & Ghosh, T. (2010). Darkness on the edge of town: Mapping urban and peri-urban Australia using nighttime satellite imagery. *The Professional Geographer*, 62(1), 119–133.
- Torres-Valcárcel, Á. R., Harbor, J., Torres-Valcárcel, A. L., & González-Avilés, C. J. (2014). Historical differences in temperature between urban and non-urban areas in Puerto Rico. *International Journal of Climatology* <<http://dx.doi.org/10.1002/joc.4083>>.
- United Nations (2012). World urbanization prospects: The 2011 revision highlights. <<http://www.slideshare.net/undesa/wup2011-highlights>>.
- White, H. (1980). A heteroskedasticity-consistent covariance matrix estimator and a direct test for heteroskedasticity. *Econometrica*, 48(4), 817–838.
- Wickham, J. D., Stehman, S. V., Gass, L., Dewitz, J., Fry, J. A., & Wade, T. G. (2013). Accuracy assessment of NLCD 2006 land cover and impervious surface. *Remote Sensing of Environment*, 130, 294–304.
- Wolters, D., & Brandsma, T. (2012). Estimating urban heat island in residential areas in the Netherlands using observations by weather amateurs. *Journal of Applied Meteorology and Climatology*, 51(4), 711–721.
- Wong, M. S., Nichol, J. E., To, P. H., & Wang, J. (2010). A simple method for designation of urban ventilation corridors and its application to urban heat island analysis. *Building and Environment*, 45(8), 1880–1889.
- Zhou, B., Rybski, D., & Kropp, J. P. (2013). On the statistics of urban heat island intensity. *Geophysical Research Letters*, 40(20), 5486–5491.
- Zhou, Y., & Shepherd, J. M. (2010). Atlanta's urban heat island under extreme heat conditions and potential mitigation strategies. *Natural Hazards*, 52(3), 639–668.